2021

Truss Bridge Damage Localization and Severity Estimation Using Influence Lines

Hamoud Alshallaqi
h.alshallaqi@gmail.com

TRUSS BRIDGE DAMAGE LOCALIZATION AND SEVERITY ESTIMATION

USING INFLUENCE LINES

Approved by:

_____

Dr. Brett A. Story
Associate Professor, Civil and Environmental Engineering

_____

Dr. Nicos Makris
Addy Family Centennial Professor of Civil Engineering

_____

Dr. Usama El Shamy
Associate Professor, Civil and Environmental Engineering

TRUSS BRIDGE DAMAGE LOCALIZATION AND SEVERITY ESTIMATION USING INFLUENCE LINES

A Thesis Presented to the Graduate Faculty of the

Bobby B. Lyle School of Engineering

Southern Methodist University

in

Partial Fulfillment of the Requirements

for the degree of

Master of science

In

Civil Engineering

with a

Specialization in Structural Engineering
by

Hamoud Hamad Alshallaqi

B.S., Civil Engineering, University of Ha'il

December 18, 2021

Hamoud Hamad Alshallaqi B.S., Civil Engineering, University of Ha'il, 2017

Truss Bridge Damage Localization and
Severity Estimation Using Influence Lines

Advisor: Dr. Brett Story

Master of Science conferred December 18, 2021

Thesis completed December 1, 2021

The safety of bridges is one of the primary concerns of researchers, engineers, and bridge owners and managers, especially when bridges are approaching the end of their intended service lives. The estimation of bridge condition and remaining service life is critical to prioritize the allocation of available funding for repairs and rehabilitation. Various methods, including both dynamic and static approaches, have been developed to detect and localize bridge damage and estimate its severity. This research presents a methodology for detecting a single damaged member in a truss bridge and estimating the severity of the damage using static vertical deflection influence lines (SDILs). The methodology is capable of making assessments using fewer sensors and measurement locations than other state of the art methodologies, thereby minimizing costs and service interruptions to bridge owners. This work comprises the development of the methodology and a parametric study to determine the sensitivity of the methodology to uncertainties faced in practice. The results show that the proposed methodology is able to identify the damaged member and estimate damage severity; performance results are given for various combination of measurement noise levels, number of simulations, and damage severities.

TABLE OF CONTENTS

LIST OF TABLES

LIST OF FIGURES

ACKNOWLEDGMENTS

First and foremost, I would like to express my sincere gratitude to my advisor, Dr. Brett Story, for his patience, encouragement, motivation, and unlimited support throughout my master's study. I am grateful for the time he took to listen to the problems I faced and advise me during my thesis work. His advice and supervision have given insight for both my academic and personal life. Thank you, Dr. Story, for being a knowledgeable and encouraging mentor and advisor.

I also want to thank my committee members, Drs. Usama El Shamy and Nicos Makris, for their willingness to serve as members in my thesis defense committee and for taking the time to review and provide their guidance and support throughout this project.

My thanks go to my friends for helping and always being around to listen, encourage, and motivate. A special thanks goes to my colleague Jase Sitton for helping me with various aspects of my thesis work.

Last but certainly not least, I would like to express my deepest gratitude to my parents, Hamad and Feriha, and to my siblings. I know it is hard for you that I am far away from home. Despite the distance, you all have always been with me. Thanks for being there whenever I need to call and chat and believing in me. None of what I have accomplished and achieved in both my academic and personal life would be possible without you all.

CHAPTER 1

INTRODUCTION

1.1 Background

Many bridges in the United States are approaching or exceeding their intended service life [1]. According to the 2021 Report Card for America's Infrastructure published by ASCE, there are over 600,000 bridges in the U.S., with U.S. bridge infrastructure receiving an overall grade of C. ASCE reports that 42% of U.S. bridges are over 50 years old; the average age of a bridge in the U.S. is 44 years. Around 46,150 nation's bridges are classified as structurally deficient [1]. Therefore, it is essential to monitor their condition to prevent bridge failures, decrease risks, and plan maintenance for each bridge. It is estimated that $125 billion is required for the nation's bridge repair backlog [1].

In recent decades, structural health monitoring (SHM) systems have emerged as important tools in monitoring existing structural systems; many research efforts have focused on developing SHM methodologies for different applications [2-12, 17-34]. Automated SHM systems provide real-time evaluation of structural health for existing infrastructure so that decision-makers can stay updated about infrastructure performance and integrity and early decisions can be made to prevent catastrophic failure or interruption of service. Additionally, SHM systems may reduce the cost of unnecessary maintenance and permit optimized scheduling of required maintenance.

1.2 Problem Statement

In light of aging infrastructure, an opportunity exists to develop cost-effective and practicable approaches to monitor structural systems. This research presents a method to monitor truss bridge members with relatively few sensors by using the static deflection influence lines (SDILs) of bottom chord joints.

Specifically, the objectives of this work are:

1. Develop an influence line-based method that is capable of localizing damage in a truss system and estimating the severity of the damage
2. Examine how the developed method performs with the addition of noise
3. Determine the conditions in which the method will produce acceptable results

CHAPTER 2

LITERATURE REVIEW

2.1 United States Bridge Infrastructure

According to the 2021 Report Card for America's Infrastructure published by ASCE, many bridges in the USA are approaching or exceeding their intended service lives [1]. The deterioration rate of America's bridges is greater than the rate of repair, replacement, and rehabilitation [1]. 42% of the nation's highway bridges are already exceeded their intended design lives, which increases the concern for rehabilitation or replacement [1]. It is predicted that it will take roughly 50 years to repair all of these bridges, with the estimated repair backlog of the nation's bridges totaling to 125 billion [1]. It is crucial to estimate bridge conditions to prevent failures, decrease risks, and plan maintenance for each bridge.

2.2 Visual Inspection

In 1971, the National Bridge Inspection was implemented, and since that time the visual inspection has been the most popular nondestructive evaluation technique in the United States [13, 14]. In investigation was conducted by the Federal Highway Administration's nondestructive validation center to examine the reliability of the visual inspection method [13]. The study showed that bridge health assessments vary based on bridge inspector; this may be due to several factors, including variation in inspector skills, subjective

interpretations, color vision deficiency, visual impairment, accessibility, and fear of traffic [13, 14].

Additionally, visual inspections can be costly and labor-intensive and demand long inspection times [13, 14]. Bridge inspections are scheduled at a minimum every 4 years after each inspection based on factors such as the bridge's health conditions and traffic volume [1]. In order to improve and enhance evaluation and maintenance of bridge safety, there is a need for a system that keeps decision-makers updated and reported about the health and integrity of the structure. These associated limitations and challenges have resulted in the development Structural Health Monitoring system [2].

2.3 Methods in Structural Health Monitoring

Several methods for damage identification for truss bridges have been developed recently [2-12, 17-34]. SHM algorithms are commonly classified into four levels as follows: at level 1 the algorithm should provide a general damage indication, while in levels 2, 3, and 4 the algorithm should provide additional information regarding to the location, severity, and remaining service life of the structure, respectively [15].

Currently, parameter-based identification methods are considered as one of the most important fields within SHM; these methods rely on correlating changes in test results to changes in structural properties [11]. Existing damage identification methods may be divided into two categories: static identification methods and dynamic identification methods [11]. These methods are typically validated on numerical or scale models, however some techniques have been tested on real-life bridges [3-5].

2.3.1 Dynamic Methods

Brunell and Kim investigated the effect of local damage on the overall performance of a steel truss bridge. A numerical model was developed to validate results from the physical scale model. Different technical aspects are investigated, including damage evaluation using a damage index, modal analysis, load rating, variation of strain energy, and structural safety. The results showed that the presence of the local damage significantly impacts the bridge response (i.e., deflection), especially when the damage index is greater than 0.5. Results from a dynamic analysis aspect showed that it was noticeable that the natural frequency of the 4^{th} mode decreased as the damage index increased, showing the effect of the local damage on the overall system behavior and the ability to detect it [16].

Guo proposed a fusion technique in order to increase the accuracy of localizing multiple damages based on the data from bridge response frequencies and mode shapes. A frequency change damage detection method (FCDDM) and multiple damage location assurance criterion (MDLAC) were utilized to obtain the local decision; these local decisions are then transferred to the fusion center. In the fusion center, three approaches are used to combine the data and achieve higher overall accuracy: Bayesian fusion, Dempster–Shafer evidence theory, and the fuzzy fusion method. From the fusion center, a global decision is obtained. The analysis and numerical examples showed that identification results from the fusion methods are more accurate than those from MDLAC and FCDDM independently in both damage cases [6].

Vibration-based methods have been used widely in SHM for truss bridges [3, 7-8], however these methods often rely on having large numbers of sensors installed on the

bridge, leading to financial constraints and a tradeoff between damage detection ability and monitoring cost [7].

2.3.2 Static Methods

Damage in truss structure cannot be detected by curvature methods or other methods that rely on flexural response because truss members experience predominantly axial forces and are connected by pin joints that minimize flexural demands on members; therefore, damage identification methods for truss structures should be based on the changes in axial deformation, strain energy, and stress [12].

Boumechra proposed a damage identification method based on inverse analysis of the static deflection of the bridge due to moving load. Based on a finite element model, the proposed method was able to identify reductions and changes in stiffness [9].

Jang et al used a damage locating vector (DLV) to identify a damage on a laboratory-scale truss bridge; the proposed method was capable of locating damaged members without the damaged member being instrumented [10].

Lee et al proposed a damage identification method utilizing axial stress and strain energy; the static equilibrium equation in the damaged structure can be derived by calculating changes in axial stress, strain energy, and stiffness of the structure before and after the damage, and then several damage in truss can be detected using field monitoring data contaminated with noise. The efficiency the proposed method is enhanced by the partition of the damage-expected substructure and the displacement measurements at the boundary of the partitioned subsystem [12].

2.4 Influence Line-Based Methods

An influence line is a response function that shows the amplitude variation of a structural response (e.g. axial force, shear force, bending moment, deflection, etc.) at a given point on the system structure due to the application of a static load pattern placed on any point on the structure; an influence line is referred to as a unit influence line if the load pattern is limited to a unit load [17-18]. Recently, several studies have proposed damage identification methods utilizing influence lines, such as stress influence lines [19-20], strain influence lines [21-25], and global deformation influence lines [17-18, 26-28]. Other researchers have proposed damage localization methods based on the analysis of the absolute differences between the curvatures of the deflection influence lines for damaged and undamaged beam structures [29-32].

In this study, a theoretical framework using static vertical deflection influence lines (SDILs) of the bottom chord joints of a truss bridge for damage localization and severity estimation is proposed. Utilizing the normalized absolute differences between the SDILs of damaged and intact truss bridges along with the absolute normalized axial force influence lines of truss elements, the proposed technique is able to characterize both the location and the severity of damage, with performance dependent on noise level, damage severity, and the number of simulations used to make an assessment.

CHAPTER 3

PROCEDURE AND METHODOLOGY

3.1 Theoretical derivations

The proposed method utilizes the static deflection influence lines (SDILs) of the bottom chord joints and axial force influence lines (AFILs) of truss members to localize a single damaged member and estimate damage severity. An overview of the proposed procedure is shown in Figure 1.

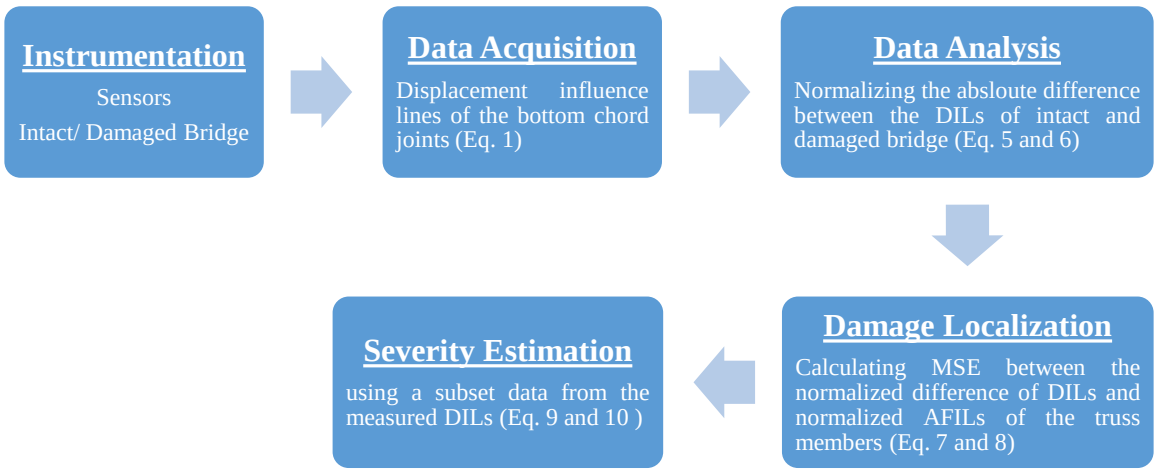

Figure 1 A flow chart showing the damage localization and severity estimation method using influence lines

The mechanical motivation for using the influence line-based method is as follows:

1. Damage in truss members may manifest as a change in axial stiffness
2. Change in axial stiffness in a truss member affect its contribution to the deflection of any of the bottom chord joints
3. Not all the truss members have the same normalized axial force influence lines

The structure is assumed to be elastic. The moving load intensity in both damaged and intact states is the same and its dynamic impact is neglected. The normalized AFILs are assumed to be calculated through basic truss analysis. The geometry of the truss bridge is assumed to be known and the truss self-weight is neglected.

3.1.1 Damage Localization

First, the SDILs of the bottom chord joints of the intact bridge are calculated. The DILs of the bottom cord joints based on the method of virtual work can be written as shown in Equation 1:

$$\Delta = FK^{-1}Q = \begin{bmatrix} \Delta_{11} & \cdots & \Delta_{1n} \\ \vdots & \ddots & \vdots \\ \Delta_{j1} & \cdots & \Delta_{jn} \end{bmatrix} \quad (1)$$

where

- Δ is a [*J*N*] matrix representing the DILs of the bottom chord joints
- *F* is a [*J*M*] matrix representing the AFILs for the truss members due to a real moving load
- *K* is a [*M*M*] diagonal matrix where the diagonal entries represent the axial stiffnesses of the truss members

- *Q* is a [*M*N*] matrix representing the AFILs of the truss members due to a moving unit load

J, *M*, and *N* are number of the moving load steps, number of the truss members, and number of the bottom chord joints, respectively.

j, *m*, and *n* are location of the moving load, member, and location of the measurements respectively.

The matrices *Q*, *K*, and *F* can be written as shown in Equations 2, 3, and 4, respectively

$$\mathrm{Q} = \mathrm{I} * \mathrm{C} = \begin{bmatrix} 1 & \cdots & 0 \\ \vdots & \ddots & \vdots \\ 0 & \cdots & 1 \end{bmatrix} * \begin{bmatrix} c_{11} & \cdots & c_{1n} \\ \vdots & \ddots & \vdots \\ c_{m1} & \cdots & c_{mn} \end{bmatrix} \quad (2)$$

$$K = \begin{bmatrix} K_1 & \cdots & 0 \\ \vdots & \ddots & \vdots \\ 0 & \cdots & K_m \end{bmatrix} \quad (3)$$

$$F = P * C^T = \begin{bmatrix} P_{1(x1)} & \cdots & P_{n(x1)} \\ \vdots & \ddots & \vdots \\ P_{1(xj)} & \cdots & P_{n(xj)} \end{bmatrix} * \begin{bmatrix} c_{11} & \cdots & c_{1n} \\ \vdots & \ddots & \vdots \\ c_{m1} & \cdots & c_{mn} \end{bmatrix}^T \quad (4)$$

where

- *C* is [*M*N*] matrix represents the influence line coefficients for the truss members
- *I* is the [*N*N*] identity matrix x_j is the location of the moving load
- $P_{n(xj)}$ is the amount of the moving load transferred to joint n when the load is at x_j

The difference between the damaged and intact SDILs of the bottom chord joints is obtained by Equation 5:

$$\Delta' = \Delta^d - \Delta \tag{5}$$

Here, Δ' is the difference between the damaged and intact SDILs of the bottom chord joints and Δ^d is the SDIL of the damaged bridge.

By taking the absolute value of the difference between the damaged and intact SDILs of a bottom chord joint and then normalize it with respect to the maximum absolute value of the deflection, the absolute normalized difference between the SDILs of the intact and damaged bridge is obtained as shown in Equation 6:

$$\overline{\Delta'_n} = \frac{|\Delta'_n|}{\max(|\Delta'_n|)} = \begin{bmatrix} \overline{\Delta'_{1n}} \\ \vdots \\ \overline{\Delta'_{jn}} \end{bmatrix} \tag{6}$$

The absolute normalized AFILs of each truss member with respect to the maximum absolute axial force in a given member can be calculated using the AFILs coefficients:

$$\overline{F_m} = \frac{|C_m|}{\max(|C_m|)} = \begin{bmatrix} \overline{F_{1m}} \\ \vdots \\ \overline{F_{jm}} \end{bmatrix} \tag{7}$$

Here, $\overline{F_m}$ and C_m are the normalized AFIL of member *m* and the coefficients influence lines of member *m*, respectively.

Suppose damage occurs in one of the members; in that case, the Mean Squared Error (MSE) of the normalized difference SDILs of a bottom chord joint and the normalized AFIL of the damaged member is expected to be small because $\overline{\Delta'_n}$ is equal to $\overline{F_m}$ for the

damaged member. In contrast, the other members are expected to have much higher values of MSE. Therefore, the damaged member can be identified by calculating the MSE of the absolute difference between the normalized SDILs of one of the bottom chord joints and the normalized AFILs of the truss members is as shown in Equation 8.

$$\text{MSE} = \frac{1}{J}\sum_{j=1}^{J}\left(\overline{F_{jm}} - \overline{\Delta'_{jn}}\right)^2 \tag{8}$$

The member with the lowest value of MSE is identified as the damaged member.

3.1.2 Severity Estimation

After identifying the damaged member and using prior knowledge of its AFILs from a finite element model in conjunction with the method of virtual work, the ratio of the contribution of the damaged member to the deflection of the bottom chord joints in an intact state is calculated using Equation 9.

$$CR_{jnm} = \frac{\left(\frac{F_{jm}Q_{mn}}{k_m}\right)}{\Delta_{jn}^{c}} \tag{9}$$

CR_{jnm} represents the contribution ratio of the axial displacement of member m to the vertical deflections of joint n when the real moving load is at j and Δ_{jn}^{c} is the calculated vertical displacement. CR_{jnm} can be numerically computed either by assuming the moving load equal is a unit load or by using the influence line coeffecients. The contribution ratios are then used to estimate the severity of the damage as shown in Equation 10.

$$SE\%_m = \left(1 - \frac{CR_{jnm} * \Delta_{jn}}{\left(CR_{jnm} * \Delta_{jn} + \Delta'_{jn}\right)}\right) * 100 \tag{10}$$

3.2 Truss Members Classifications

Multiple members may have the same normalized AFILs, so these members are classified as one group. If damage occurs in one member or multiple members from the same group, MSE will indicate damage in all group members.

CHAPTER 4

ANALYTICAL MODEL

4.1 Truss Bridge Model

This section describes finite element models of two different bridge configurations used to evaluate the proposed truss bridge damage localization and severity estimation methodology using influence lines. The first 2D model is a simple truss bridge, shown in Figure 2a, which comprises nine truss elements and two bottom cord joints. All truss members in Model 1 are steel with a modulus of elasticity of 29000 ksi. Vertical and horizontal members have a length of 17.5 ft; the diagonal member is 24.75 ft. The cross-sectional area of all elements is 22 in^2. The second 2D model, shown in Figure 2b, is a warren truss with vertical members and a span of 120 ft divided into six equal parts with a height of 17 ft. All truss members are steel with a modulus of elasticity of 29000 ksi. Table 1 lists member cross-sections for Model 2.

Both models have pinned connections at the joints and are simply supported. In practice, using fewer sensors facilitates more economical and efficient operation, i.e. instrumenting every joint in the field may not be practical. In this study, the displacements of all of the bottom chord joints are recorded in both models in order to assess the accuracy and investigate the sensitivity of each joint to the damage location. SAP2000 is utilized to show and visualize the analyzed truss bridges

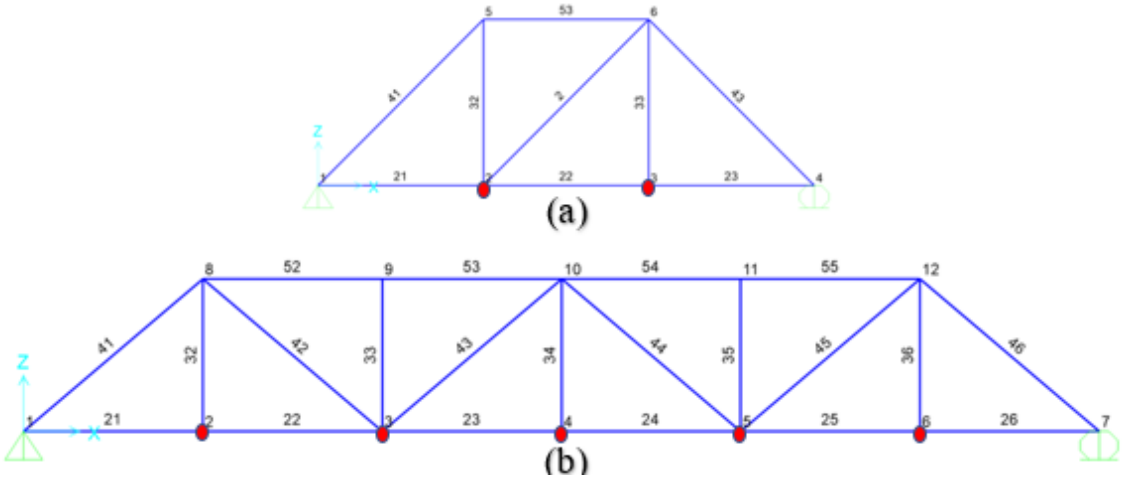

Figure 2. 2D Truss bridge models (recorded joints are marked with red dots): (a) Model 1, (b) Model 2

In this study, the vertical displacements of all the bottom chord joints in both models are recorded, as shown in Figure 2. However, the proposed method can locate the damage and estimate the severity by using results from a complete and subset recorded SDILs, respectively.

Table 1 Steel sections of Model 2

Section type	Bridge component	Dimensions (in)
W-Shape (W30×173)	Bottom chords	Outside height = 30.4 Flange width = 15 Flange thickness = 1.07 Web thickness = 0.655
W-Shape (W21×122)	Vertical & top chords	Outside height = 21.7 Flange width = 12.4 Flange thickness = 0.960 Web thickness = 0.600
Hollow structural section (HSS16×16×$^{5}/_{8}$)	Diagonals	Outside depth and width = 16 Flange and web thickness = 0.581

4.2 Damage Cases

In this section, different damage cases and damage severity levels are considered for both models. Damage is simulated through a reduction in the cross-sectional area of one member. An element is selected from different element groups for each damage case in both models. The damage locations and severity levels for Models 1 and 2 are listed in Tables 2 and 3, respectively, and are shown visually in Figures 3 and 4, respectively.

Table 2 Damage cases for Model 1

Damage case	Damage location and severity levels
DC-1	Element 22: cross-section damage by (a) 15% (b) 35%
DC-2	Element 42: cross-section damage by (a) 15% (b) 35%
DC-3	Element 53: cross-section damage by (a) 15% (b) 35%

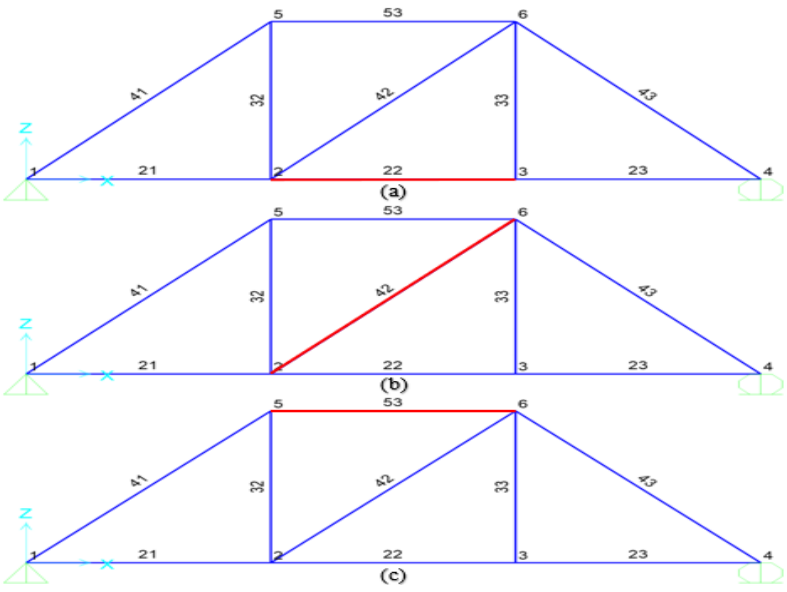

Figure 3 Damage cases analyzed for Model 1: (a) damage case 1, (b) damage case 2, (c) damage case 3

Table 3 Damage cases for Model 2

Damage case	Damage location and severity levels
DC-1	Element 41: cross-section damage by (a) 15% (b) 35%
DC-2	Element 53: cross-section damage by (a) 15% (b) 35%
DC-3	Element 43: cross-section damage by (a) 15% (b) 35%
DC-4	Element 23: cross-section damage by (a) 15% (b) 35%

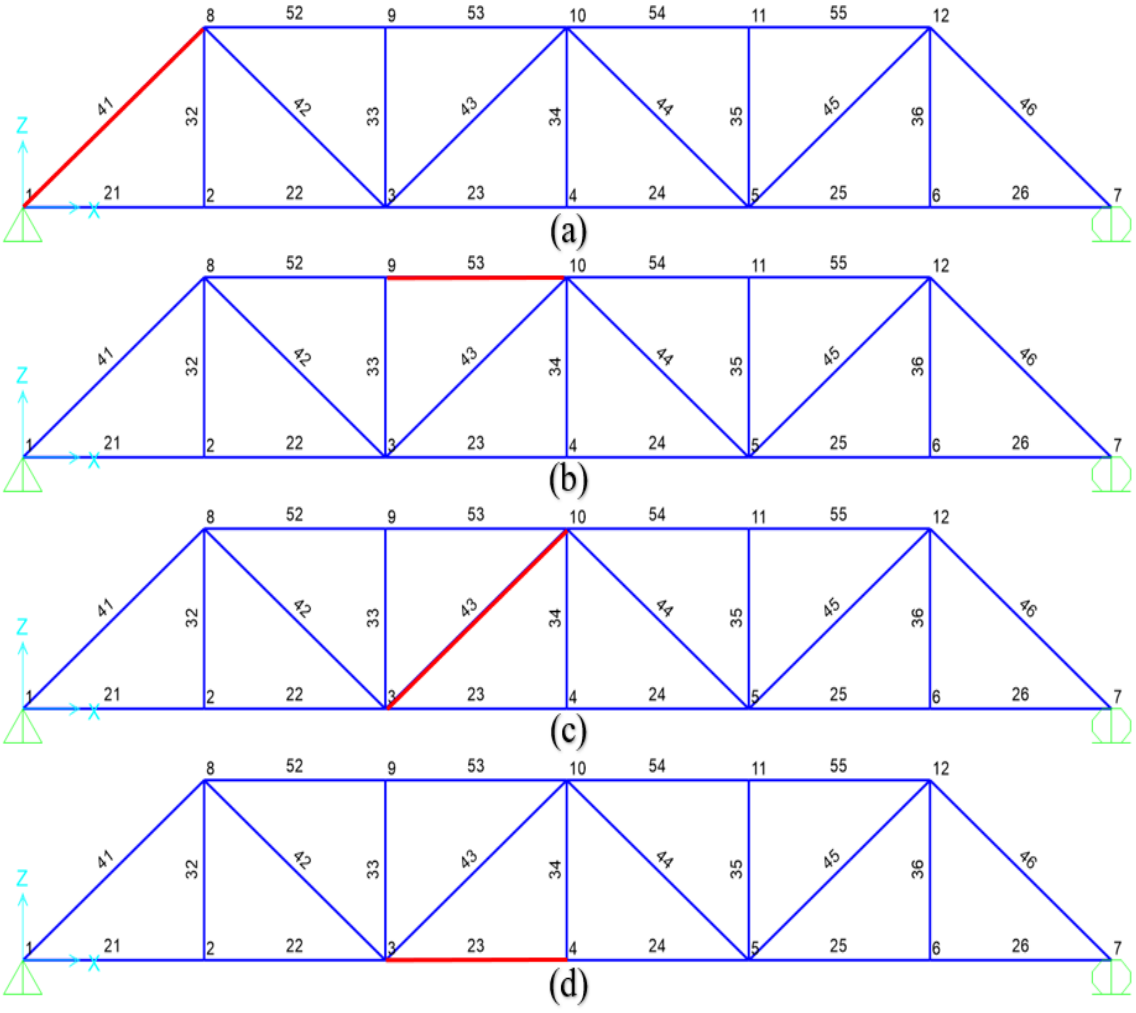

Figure 4 Damage cases analyzed for Model 2: (a) damage case 1, (b) damage case 2, (c) damage case 3, (d) damage cas

CHAPTER 5

RESULTS AND DISCUSSION

5.1 Truss Member Classification

As discussed in Chapter 3, multiple members may have the same normalized AFILs. Therefore, members are grouped based on the similarity of their normalized AFILs. If damage occurs in one or multiple members from the same group, the proposed method will indicate damage in all the elements in that group. Nevertheless, members with the same normalized AFILs may have different contributions to the deflection of bottom chord joints, affecting the accuracy of the proposed detection method. Truss members for Models 1 and 2 are grouped using the AFILs coefficients as shown in Tables 4 and 5, respectively.

Table 4 Truss members groups for Model 1

Group No.	Truss members
G-1	Elements: 21, 32, 41, and 53
G-2	Elements: 22, 23, and 43
G-3	Elements: 33
G-4	Elements: 42

Truss members of Model 1 are grouped into 4 groups. Elements 33 and 42 have unique normalized AFILs.

Table 5 Truss members groups for Model 2

Group No.	Truss members
G-1	Elements: 21, 22, and 41
G-2	Elements: 23 and 24
G-3	Elements: 25, 26, and 46
G-4	Elements: 32
G-5	Elements: 34
G-6	Elements: 36
G-7	Elements: 42
G-8	Elements: 43
G-9	Elements: 44
G-10	Elements: 45
G-11	Elements: 52 and 53
G-12	Elements: 54 and 54

Table 5 shows that, as the truss geometry complexity increases, more members exhibit unique normalized AFILs. 7 groups out of 12 have only one member in each with a unique normalized AFIL among other members. Members 33 and 35 are neglected since they are zero-force members.

5.2 Damage Cases Analysis and Results

In this section, multiple damage cases, which are shown in Tables 2 and 3, are investigated for Model 1 and Model 2. In practical cases, the displacement measurements are contaminated by noise due to various factors, including measuring equipment, measurement reading, and so on [9]. Therefore, to more closely simulate a real-life test, several error types can be added into the displacements data to simulate noise [11]. Two

common types of random error used to simulate noise in measurements are uniform error and error following a normal distribution [11]. To assess the efficiency of the proposed method, proportional uniform noise is added to the calculated DILs with different magnitude noise levels for both damaged and undamaged structures. Noise is added to DIL data by using the following [33]:

$$\Delta_{noisy} = \Delta_{noise-free} * (1 + \varepsilon * R) \quad (11)$$

Where the parameter ε represents the level of noise and R is a matrix that has the same size as the $\Delta_{noise-free}$. Matrix R contains random numbers in the range [-1 1]. Increasing the number of the moving load steps and measurements simulations leads to more accurate results and reduces noise's effect [9]. Therefore, the moving load step is assumed to be 0.5 ft for both models. The measurement simulations are assumed to be 1, 10, 20, and 30 for both models, where each simulation has a complete recorded SDILs. The amplitude of the moving load is considered to be 35 kips, and all calculated DILs are polluted with noise levels 1%, 2%, 3%, 4%, and 5%.

In the results tables, cases with an accuracy of less than 50% are shown as a dash meaning no decision. To increase the accuracy of the severity estimation, a subset of displacements data is selected based on the location of the damaged member and its contributions to the displacement of the bottom chord joints, and that can be illustrated by using the plot of the absolute difference between the damaged and intact DILs with noise level = 0, e.g., Figure 5. Moreover, the plot also shows the most sensitive bottom chord joint to the damaged member that provides accurate severity estimations among other bottom chord joints. However, it can be calculated regardless of the measured data using

the AFILs coefficients. In case there is damage in one member from a classified group of members, the severity estimation of the intact members should be equal to the damaged member when they have the same axial stiffness; otherwise, the estimation would vary based on the difference between their axial stiffnesses.

Theoretically, the normalized difference between the intact and damaged SDILs of all the bottom cord joints is similar, so an assessment procedure using the average of the normalized difference of DILs of all the bottom chord joints is utilized. All the shown results are based on the average of multiple iterations. All calculations in this study are performed using MATLAB code; deflection values are rounded to the thousandths place.

5.2.1 Model 1 Results and Discussions

5.2.1.1 Cross-Section Damage in Element 22: DC-1 Model 1

In this damage case, Element 22, shown in Figure 3a, is damaged due to a reduction in the cross-sectional area by 15% and 35%, along the entire length. The location of the maximum contribution from Element 22 is when the moving load at Joint 3, as shown in Figure 5; Joint 3 is more sensitive to the damaged member than Joint 2. The specific cases shown in Figures 6a and 6b were selected with the noise level, simulations, and percentage of damages of 2%, 30, 15%, and 35%, respectively, to illustrate damage localization.

It can be observed from Figure 6a that if the displacement data of Joint 3 is used, the proposed method accurately identifies Members 22, 23, and 43 as damaged members; these members belong to the same group in Table 5. Estimation using Joint 2 and the average erroneously indicate damage in member 33; Joint 2 is ineffective in detecting damage in members from group G-2. Figure 6bshows that when the percentage of the damage

increased to 35%, the method identified a damage in G-2 members using both joints, demonstrating that the accuracy of all joints increases as the damage percentage increases due to the increase in the contribution of the element 22.

Tables 6, 7, and 8 show the accuracy of the proposed damage localization method. The assessment method using the data from Joint 3 was capable of locating the damage with 15% and 30% severity for some number of simulations and some levels of noise. The severity of the damage is assessed two times; first by using complete joint displacement data followed by using a subset of joint displacement data. As mentioned previously, the accuracy of the severity estimation can be enhanced by selecting a subset of data based on the location of the maximum contribution, as shown in Figure 5; therefore, the selected displacement data is when the moving load in between 17.5 to 45 ft away from the left support. The selected subset data showed a significant improvement in the severity evaluation for both joints, as shown in tables 9-12.

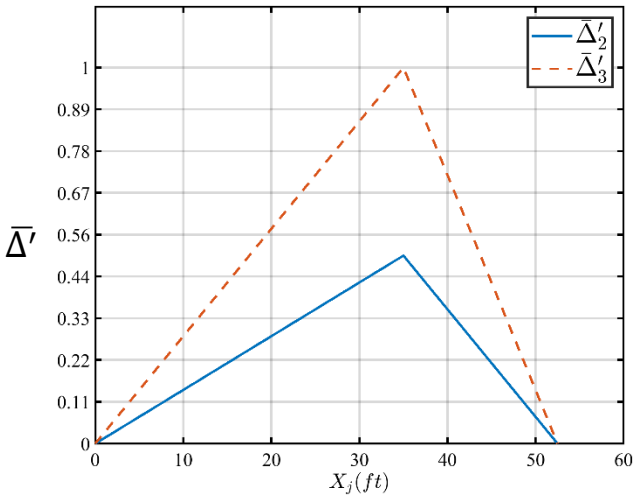

Figure 5 Location of the maximum contribution from the damaged member to the bottom chord joints (DC-1, Model 1)

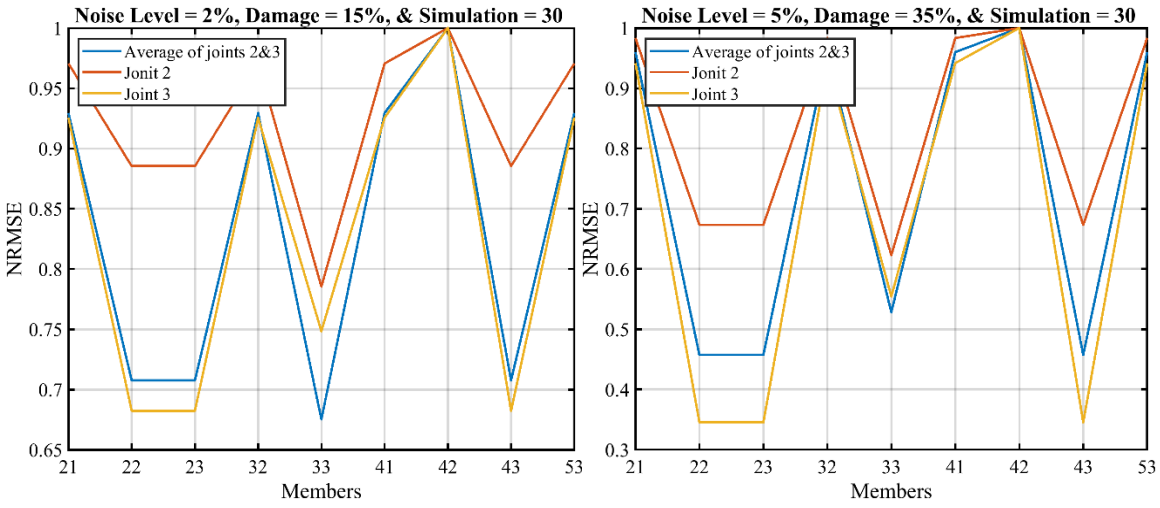

(a) (b)

Figure 6 Damage localization for DC-1: (a) N = 2%, Damage = 15% and simulations = 30 (b) N = 2% Damage = 35% and simulations = 30 (DC-1, Model 1)

Table 6 Accuracy of the assessment using Joint 2 (DC-1, Model 1)

Simulation	Accuracy of the assessment using Joint 2 (%)									
	Damage = 15%					Damage = 35%				
	ε (%)					ε (%)				
	1	2	3	4	5	1	2	3	4	5
1	-	-	-	-	-	51.1	-	-	-	-
10	-	-	-	-	-	72.3	54.6	53.4	-	-
20	-	-	-	-	-	80.3	61.4	56.8	53.3	50
30	-	-	-	-	-	84.7	66.5	58.9	54.1	52.6

Table 7 Accuracy of the assessment using Joint 3 (DC-1, Model 1)

Simulation	Accuracy of the assessment using Joint 3 (%)									
	Damage = 15%					Damage = 35%				
	ε (%)					ε (%)				
	1	2	3	4	5	1	2	3	4	5
1	-	-	-	-	-	99.9	-	-	-	-
10	99.9	75.1	-	-	-	100	100	98.9	88.5	72.3
20	100	93.9	69.4	-	-	100	100	100	99.3	95
30	100	98.6	85.7	59.9	-	100	100	100	100	98.5

Table 8 Accuracy of the assessment using the average of Joints 2 and 3 (DC-1, Model 1)

Simulation	Accuracy of the assessment using average of Joint 2&3 (%)									
	Damage = 15%					Damage = 35%				
	ε (%)					ε (%)				
	1	2	3	4	5	1	2	3	4	5
1	-	-	-	-	-	95.8	50.3	-	-	-
10	-	-	-	-	-	100	99.9	94.2	77.1	62.7
20	-	-	-	-	-	100	100	99.6	95.7	85.3
30	-	-	-	-	-	100	100	100	99.2	94.3

Table 9 The Average of the severity estimation Joint 2 (complete data , DC-1, Model 1)

Simulation	The Average of the severity estimation Joint 2 (%)									
	Damage = 15%					Damage = 35%				
	ε (%)					ε (%)				
	1	2	3	4	5	1	2	3	4	5
1	-	-	-	-	-	24.6	-	-	-	-
10	-	-	-	-	-	26.5	25.9	24.7	-	-
20	-	-	-	-	-	26.6	26.3	25.8	25	24.1
30	-	-	-	-	-	26.6	26.4	26.1	25.6	24.9

Table 10 The Average of the severity estimation Joint 3 (complete data, DC-1, Model 1)

Simulation	The Average of the severity estimation Joint 3 (%)									
	Damage = 15%					Damage = 35%				
	ε (%)					ε (%)				
	1	2	3	4	5	1	2	3	4	5
1	-	-	-	-	-	30.4	-	-	-	-
10	12.1	12	-	-	-	30.6	30.6	30.5	30.3	30.1
20	12.2	12.1	12	-	-	30.6	30.6	30.6	30.5	30.4
30	12.2	12.1	12.1	12	-	30.6	30.6	30.6	30.5	30.5

Table 11 The Average of the severity estimation Joint 2 (subset data, DC-1, Model 1)

Simulation	The Average of the severity estimation Joint 2 (%)									
	Damage = 15%					Damage = 35%				
	ε (%)					ε (%)				
	1	2	3	4	5	1	2	3	4	5
1	-	-	-	-	-	32.1	-	-	-	-
10	-	-	-	-	-	32.3	32.2	32.1	-	-
20	-	-	-	-	-	32.3	32.3	32.2	32.1	32
30	-	-	-	-	-	32.3	32.3	32.2	32.2	32.1

Table 12 The Average of the severity estimation Joint 3 (subset data, DC-1, Model 1)

Simulation	The Average of the severity estimation Joint 3 (%)									
	Damage = 15%					Damage = 35%				
	ε (%)					ε (%)				
	1	2	3	4	5	1	2	3	4	5
1	-	-	-	-	-	33.8	-	-	-	-
10	13	12.9	-	-	-	34	33.9	33.8	33.7	33.5
20	13.1	13	12.9	-	-	34	33.9	33.9	33.8	33.8
30	13.1	13	13	12.9	-	34	34	33.9	33.9	33.8

5.2.1.2 Cross-Section Damage in Element 42: DC-2 Model 1

In this damage case, element 42, shown in Figure 3b, is simulated to be damaged due to a reduction in the cross-sectional area by 15% and 35%, along with the entire length. The specific cases shown in Figures 8a and 8b were selected with noise level, simulations, and percentage of damages of 4% and 3%, 30 and 1, 15% and 30%, respectively, to clarify the damage localization method. It can be clearly seen that in Figures 8a and 8b, the damaged element is accurately identified by using displacement data of Joint 2, Joint 3, and the average of joints. It is observable that at 35% damage severity, the damaged member is detected by all the assessment procedures with high levels of noise except at one simulation, as shown in tables 13, 14, and 15. It is recognizable that both joins have the same sensitivity to the impaired element, as illustrated in Figure 7. However, the severity estimations using the complete data were not reliable and repeatable because of the effect of noise on the small numbers of displacement data for both joints when the static moving load between joins 2 and 3. Therefore, the severity estimations using the complete displacement data are excluded in this damage case. Using a subset of data ranging between 10 ft to 20 ft and 32.5 ft to 42.5 ft, the severity of damage is assessed with absolute errors in between 0.9 % to 1.9 % for 15 % damage case using data from both joints. It is evident that there are minor variations between severity assessments using Joints 2 and 3 due to the effect of noise and an increase in the contribution ratio of the element 42 when the moving load between the left support and Joint 2. Overall, the damage is successfully identified and detected. The average severity is estimated by all the assessment procedures at only the damage severity of 15% and 35% regardless of at one simulation and level of noise 2, 3, 4, and 5 for 15% damage severity.

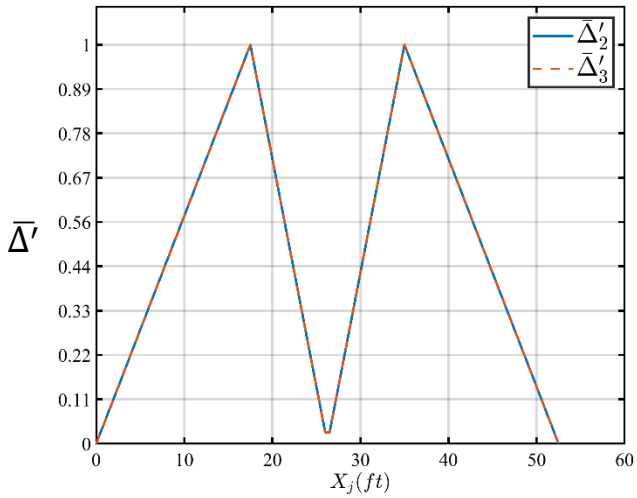

FIGURE 7 LOCATION OF THE MAXIMUM CONTRIBUTION FROM THE DAMAGED MEMBER TO THE BOTTOM CHORD JOINTS (DC-2, MODEL 1)

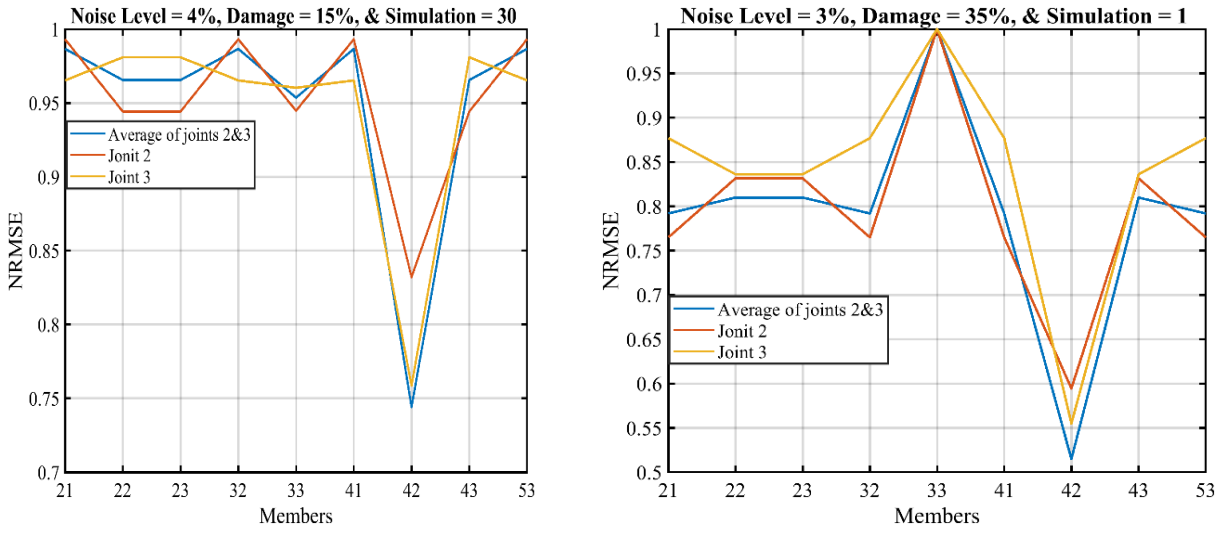

(a) (b)

Figure 8 Damage localization for DC-2: (a) N = 4%, Damage = 15% and simulations = 30 (b) N = 5% Damage = 35% and simulations = 1 (DC-2, Model 1)

Table 13 Accuracy of the assessment using Joints 2 (DC-2, Model 1)

Simulation	Accuracy of the assessment using Joint 2 (%)									
	Damage = 15%					Damage = 35%				
	ε (%)					ε (%)				
	1	2	3	4	5	1	2	3	4	5
1	91	-	-	-	-	100	100	98.3	85.2	58.9
10	100	99	89.4	71.4	55.1	100	100	100	100	100
20	100	100	97.8	91.1	79	100	100	100	100	100
30	100	100	99.8	96.5	89.6	100	100	100	100	100

Table 14 Accuracy of the assessment using Joint 3 (DC-2, Model 1)

Simulation	Accuracy of the assessment using Joint 3 (%)									
	Damage = 15%					Damage = 35%				
	ε (%)					ε (%)				
	1	2	3	4	5	1	2	3	4	5
1	96	-	-	-	-	100	100	95.3	60.8	-
10	100	100	94.5	73.2	51.5	100	100	100	100	100
20	100	100	99.6	95.9	84.2	100	100	100	100	100
30	100	100	100	99.1	94.9	100	100	100	100	100

Table 15 Accuracy of the assessment Joints 2 and 3 (DC-2, Model 1)

Simulation	Accuracy of the assessment using average of Joint 2&3 (%)									
	Damage = 15%					Damage = 35%				
	ε (%)					ε (%)				
	1	2	3	4	5	1	2	3	4	5
1	99	-	-	-	-	100	100	99.9	87.9	53.7
10	100	100	97.8	81.1	60.3	100	100	100	100	100
20	100	100	100	98.5	89.9	100	100	100	100	100
30	100	100	100	99.9	98.3	100	100	100	100	100

Table 16 The Average of the severity estimation Joint 2 (subset data, DC-2, Model 2)

Simulation	The Average of the severity estimation Joint 2 (%)									
	Damage = 15%					Damage = 35%				
	ε (%)					ε (%)				
	1	2	3	4	5	1	2	3	4	5
1	13.7	-	-	-	-	34.4	33.8	32.9	31.2	28.6
10	14	13.9	13.7	13.4	13.1	34.6	34.5	34.4	34.3	34.1
20	14.1	14	13.9	13.7	13.5	34.6	34.6	34.5	34.4	34.4
30	14.1	14	14	13.8	13.7	34.6	34.6	34.5	34.5	34.5

Table 17 The Average of the severity estimation Joint 3 (subset data, DC-2, Model 1)

Simulation	The average of the severity estimation Joint 3 (%)									
	Damage = 15%					Damage = 35%				
	ε (%)					ε (%)				
	1	2	3	4	5	1	2	3	4	5
1	13.5	-	-	-	-	34	33.2	31.7	29.2	20.3
10	14.1	13.9	13.6	13.1	12.6	34.2	34.1	34	33.9	33.6
20	14.1	14	13.9	13.6	13.4	34.2	34.2	34.1	34.1	33.9
30	14.1	14.1	14	13.8	13.6	34.2	34.2	34.2	34.1	34.1

5.2.1.3 Cross-Section Damage in Element 53: DC-3 Model 1

In this damage case, element 53, shown in Figure 3c, is simulated to be damaged due to a reduction in the cross-sectional area by 15% and 35%, along with the entire length. Based on the location of the maximum contribution, shown in Figure 9, from element 53, Joint 2 is highly sensitive to G-1. It can be observed from Figure 10a that the damage localization method using the average assessment procedure indicates to damage in G-1 even with less sensitivity of Joint 3. It is observed that with a damage severity of 35%, the damage is located using all the damage assessment procedures at the level of noise 5% and only with one simulation, as shown in Figure 10b. It is noticeable from table 19 that even with increasing the number of simulations, the severity assessments using Joint 3 at 15% severity are not accurate with high noise levels. Using a subset of displacement data, when

the moving load ranging in between 7.5 ft to 27.5 ft away from the left support, of Joint 2, decreased the average absolute error at 15% severity from (3.3 % – 6.7%) to (0.9% – 3.2%) regardless of assessments when the simulations =1 and levels of noise = 4 and 5, as shown in tables 21 and 23. The severity assessments at 35% damage severity with (simulations = 1 and N = 2, 3, 4, and 5), (simulations = 20 and N = 4, and 5), and (simulations = 30 and N = 5) are not repeatable and reliable due the effect of noise and the low sensitivity of Joint 3 to G-1. Overall, the group of the damaged member is accurately identified and relatively quantified utilizing the displacement data of Joint 2 at the severity of 15% and 35%.

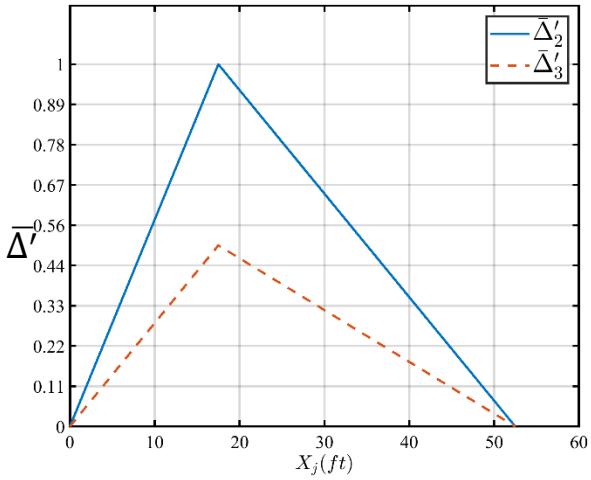

Figure 9 Location of the maximum contribution from the damaged member to the bottom chord joints (DC-3, Model 1)

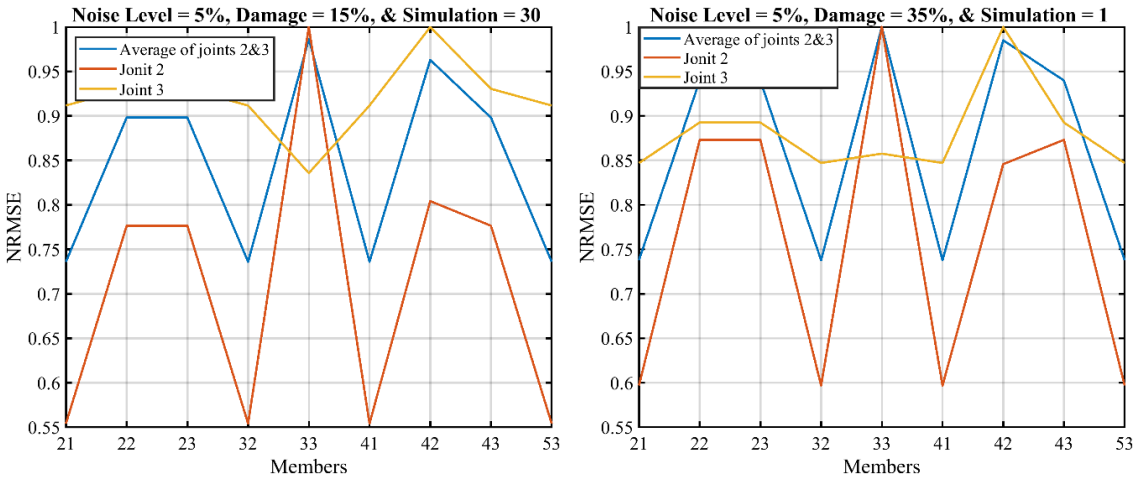

(a) (b)

Figure 10 Damage localization for DC-3: (a) N = 5%, Damage = 15% and simulations = 30 (b) N = 5% Damage = 35% and simulations = 1 (DC-3, Model 1)

Table 18 Accuracy of the assessment using Joint 2 (DC-3, Model 1)

Simulation	Accuracy of the assessment using Joint 2 (%)									
	Damage = 15%					Damage = 35%				
	ε (%)					ε (%)				
	1	2	3	4	5	1	2	3	4	5
1	100	100	93	89	87.2	100	100	100	100	99.5
10	100	100	100	100	99.9	100	100	100	100	100
20	100	100	100	100	100	100	100	100	100	100
30	100	100	100	100	100	100	100	100	100	100

Table 19 Accuracy of the assessment Joint 3 (DC-3, Model 1)

Simulation	Accuracy of the assessment using Joint 3 (%)									
	Damage = 15%					Damage = 35%				
	ε (%)					ε (%)				
	1	2	3	4	5	1	2	3	4	5
1	-	-	-	-	-	100	99.6	78.3	-	-
10	64	-	-	-	-	100	100	100	100	100
20	85	-	-	-	-	100	100	100	100	100
30	95	54.9	-	-	-	100	100	100	100	100

Table 20 Accuracy of the assessment using the average of Joint 2 & 3 (DC-3, Model 1)

Simulation	Accuracy of the assessment using average of Joint 2&3 (%)									
	Damage = 15%					Damage = 35%				
	ε (%)					ε (%)				
	1	2	3	4	5	1	2	3	4	5
1	100	69	-	-	-	100	100	100	98.6	86.4
10	100	100	100	96.9	85.2	100	100	100	100	100
20	100	100	100	100	99.2	100	100	100	100	100
30	100	100	100	100	100	100	100	100	100	100

Table 21 The Average of the severity estimation Joint 2 (complete data, DC-3, Model 1)

Simulation	The Average of the severity estimation Joint 2 (%)									
	Damage = 15%					Damage = 35%				
	ε (%)					ε (%)				
	1	2	3	4	5	1	2	3	4	5
1	11.4	10.4	8.3	5.2	0.3	32.6	32.1	31.3	30	28
10	11.7	11.6	11.4	11.1	10.9	32.8	32.7	32.6	32.5	32.4
20	11.7	11.6	11.6	11.4	11.3	32.8	32.8	32.7	32.7	32.6
30	11.7	11.7	11.6	11.5	11.4	32.8	32.8	32.7	32.7	32.7

Table 22 The Average of the severity estimation Joint 3 (complete data, DC-3, Model 1)

Simulation	The Average of the severity estimation Joint 3 (%)									
	Damage = 15%					Damage = 35%				
	ε (%)					ε (%)				
	1	2	3	4	5	1	2	3	4	5
1	-	-	-	-	-	26.2	138.	2.9	41.5	39.7
10	8.8	-	-	-	-	28.9	28.1	25.3	20.6	20.1
20	9	-	-	-	-	29	28.7	28	26.7	41.2
30	9.1	8.7	-	-	-	29.1	28.8	28.4	27.8	26.5

Table 23 The average of the severity estimation Joint 2 (subset data, DC-3, Model 1)

Simulation	The Average of the severity estimation Joint 2 (%)									
	Damage = 15%					Damage = 35%				
	ε (%)					ε (%)				
	1	2	3	4	5	1	2	3	4	5
1	13.9	13	11.8	9.5	5.9	33.2	32.8	32.1	31.1	29.7
10	14.1	14	13.9	13.8	13.5	33.3	33.3	33.2	33.1	33
20	14.1	14.1	14	13.9	13.8	33.3	33.3	33.3	33.2	33.2
30	14.1	14.1	14.1	14	14	33.3	33.3	33.3	33.3	33.2

Table 24 The average of the severity estimation Joint 2 (subset data, DC-3, Model 1)

Simulation	The Average of the severity estimation Joint 3 (%)									
	Damage = 15%					Damage = 35%				
	ε (%)					ε (%)				
	1	2	3	4	5	1	2	3	4	5
1	-	-	-	-	-	33.5	32.5	30.7	27	36.6
10	9.7	-	-	-	-	33.8	33.7	33.5	33.3	32.9
20	9.7	-	-	-	-	33.8	33.7	33.7	33.5	33.4
30	9.7	9.7	-	-	-	33.8	33.8	33.7	33.6	33.6

5.2.2 Model 2 Results and Discussions

5.2.2.1 Cross-Section Damage in element 41: DC-1 Model 2

In this damage case, element 41, shown in Figure 4a, is simulated to be damaged due to a reduction in the cross-sectional area by 15% and 35%, along with the entire length. The sensitivity of the joints to the group of the damaged member depends on how far they are from the damage location. Therefore, it can be clearly seen that the sensitivity of the joints decreases as the distance between each joint and the damage location increases, as shown in Figure 11. The damage location assessments using the average of the displacement data identify the group of the damaged member with high accuracy at some certain levels of noise and number of simulations for 15% and 35% severity, as shown in table 29. Nevertheless, the average assessment procedure advocates the damage location assessment since it is more likely to provide results close to the most sensitive joint. It is observed from Joint 2 damage assessment that the method is able to detect a damage at 5% severity with 10, 20, 30 simulations for some of the levels of noise of 1% - 2%, 1% - 3%, and 1% - 4%, respectively. The subset of displacement data is considered for (0 ft to 40 ft from the left support). Based on the considered subset data, the corresponding cases for severity estimation in Joint 2 are estimated with a maximum absolute error of 0.4%, 1.1%, and 0.5% at severity damage of 5%, 15%, and 35, respectively. Overall, the G-1 is identified and relatively quantified utilizing the displacement data of Joint 2 at some particular levels of noise and number of simulations for 15% damage severity, while it is

accurately detected and quantified at 35% severity and all levels of noise and number of simulations.

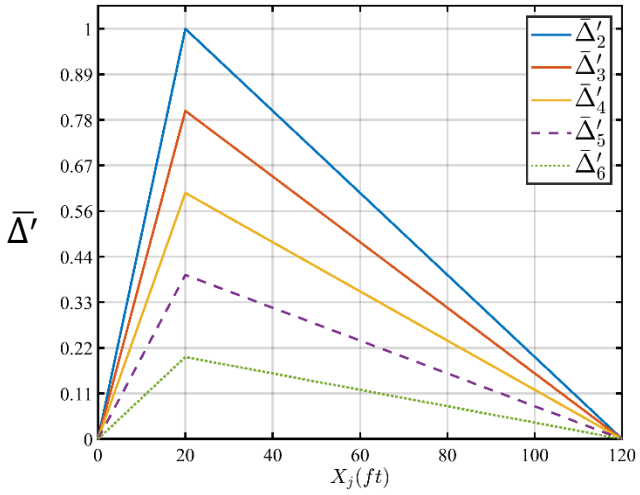

Figure 11 location of the maximum contribution from the damaged member to the bottom chord joints (DC-1, Model 2)

Table 25 Accuracy of the assessment Joint 2 (DC-1, Model 2)

Simulation	**Accuracy of the assessment using Joint 2 (%)**									
	Damage = 15%					**Damage = 35%**				
	ε (%)					**ε** (%)				
	1	**2**	**3**	**4**	**5**	**1**	**2**	**3**	**4**	**5**
1	100	91	-	-	-	100	100	100	100	100
10	100	100	100	99	97	100	100	100	100	100
20	100	100	100	100	100	100	100	100	100	100
30	100	100	100	100	100	100	100	100	100	100

Table 26 Accuracy of the assessment Joint 3 (DC-1, Model 2)

Simulation	Accuracy of the assessment using Joint 3 (%)									
	Damage = 15%					Damage = 35%				
	ε (%)					ε (%)				
	1	2	3	4	5	1	2	3	4	5
1	97	-	-	-	-	100	100	99.9	87	-
10	100	100	93.7	64	-	100	100	100	100	100
20	100	100	99.8	96	80.1	100	100	100	100	100
30	100	100	100	99	95.4	100	100	100	100	100

Table 27 Accuracy of the assessment Joint 4 (DC-1, Model 2)

Simulation	Accuracy of the assessment using Joint 4 (%)									
	Damage = 15%					Damage = 35%				
	ε (%)					ε (%)				
	1	2	3	4	5	1	2	3	4	5
1	-	-	-	-	-	100	100	81		
10	100	85	-	-	-	100	100	100	100	100
20	100	99	81	-	-	100	100	100	100	100
30	100	100	95	67.9	-	100	100	100	100	100

Table 28 Accuracy of the assessment Joint 5 (DC-1, Model2)

Simulation	Accuracy of the assessment using Joint 5 (%)									
	Damage = 15%					Damage = 35%				
	ε (%)					ε (%)				
	1	2	3	4	5	1	2	3	4	5
1	-	-	-	-	-	100	99.5			
10	97	71.8	-	-	-	100	100	100	100	98.7
20	100	88.9	62.8	-	-	100	100	100	100	100
30	100	94.8	79.4	-	-	100	100	100	100	100

Table 29 Accuracy of the assessment Joint 6 (DC-1, Model 2)

Simulation	Accuracy of the assessment using Joint 6 (%)									
	Damage = 15%					Damage = 35%				
	ε (%)					ε (%)				
	1	2	3	4	5	1	2	3	4	5
1	-	-	-	-	-	100	-	-	-	-
10	-	-	-	-	-	100	100	99.8	91.3	59.6
20	-	-	-	-	-	100	100	100	99.7	97
30	-	-	-	-	-	100	100	100	100	99.7

Table 30 Accuracy of the assessment using the average of joints (DC-1, Model 2)

Simulation	Accuracy of the assessment using average of Joint 2,3,4,5, & 6 (%)									
	Damage = 15%					Damage = 35%				
	ε (%)					ε (%)				
	1	2	3	4	5	1	2	3	4	5
1	85	-	-	-	-	100	100	100	-	-
10	100	100	76	-	-	100	100	100	100	100
20	100	100	100	89.8	-	100	100	100	100	100
30	100	100	100	99.9	85	100	100	100	100	100

Table 31 The average of the severity estimation Joint 2 (subset data, DC-1, Model 2)

Simulation	The Average of the severity estimation Joint 2 (%)									
	Damage = 15%					Damage = 35%				
	ε (%)					ε (%)				
	1	2	3	4	5	1	2	3	4	5
1	13.9	-	-	-	-	35.1	35.1	35	34.8	34.5
10	14	14	14	13.9	13.9	35.1	35.1	35.1	35.1	35.1
20	14	14	14	14	13.9	35.1	35.1	35.1	35.1	35.1
30	14	14	14	14	14	35.1	35.1	35.1	35.1	35.1

5.2.2.2 Cross-Section Damage in element 53: DC-2 Model 2

In this damage case, element 53, shown in Figure 4b, is simulated to be damaged due to a reduction in the cross-sectional area by 15% and 35%, along with the entire length. The most sensitive joint to the G-11 is Joint 3, among other joints, as shown in Figure 12. However, the accuracy of detecting the damage in element 53 is still low because the

member's contribution to the joints is low. It is clearly seen that at 15% severity and one simulation, the group of the damaged member is not detected by utilizing Joint 3 displacement data, as shown in table 32. On the other hand, using the DILs of Joint 6, the damage is detected only at 35% severity for simulation of 10, 20, and 30 and levels of noise of 1% - 2%, 1% -3%, and 1% - 4%, respectively, shown in table 35. The average of severity estimations of the corresponding considerations of the damage location using Joint 3 subset displacement data (20 ft – 60 ft away from the left support) shows accurate results with a maximum absolute error of 0.5% for damage severity of 15% and 35%, shown in table 37. Overall, the G-11 is identified and relatively quantified utilizing the displacement data of Joint 3 at some particular levels of noise and number of simulations for the severity of 15% and 35%.

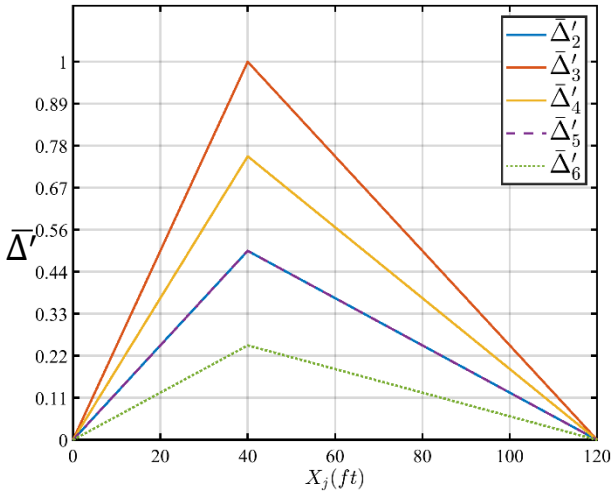

Figure 12 Location of the maximum contribution from the damaged member to the bottom chord joints (DC-2, Model 2)

Table 32 Accuracy of the assessment Joint 2 (DC-2, Model 2)

Simulation	Accuracy of the assessment using Joint 2 (%)									
	Damage = 15%					Damage = 35%				
	ε (%)					ε (%)				
	1	2	3	4	5	1	2	3	4	5
1	-	-	-	-	-	100	70	-	-	-
10	-	-	-	-	-	100	100	99.8	95.2	83.5
20	100	64	-	-	-	100	100	100	99.9	98
30	100	86	-	-	-	100	100	100	100	99.9

Table 33 Accuracy of the assessment Joint 3 (DC-2, Model 2)

Simulation	Accuracy of the assessment using Joint 3 (%)									
	Damage = 15%					Damage = 35%				
	ε (%)					ε (%)				
	1	2	3	4	5	1	2	3	4	5
1	-	-	-	-	-	100	96.1	-	-	-
10	100	65.8	-	-	-	100	100	100	99.9	98.2
20	100	93.1	60.8	-	-	100	100	100	100	100
30	100	99.3	80.9	50.6	-	100	100	100	100	100

Table 34 Accuracy of the assessment Joint 4 (DC-2, Model 2)

Simulation	Accuracy of the assessment using Joint 4 (%)									
	Damage = 15%					Damage = 35%				
	ε (%)					ε (%)				
	1	2	3	4	5	1	2	3	4	5
1	-	-	-	-	-	100	51.4	-	-	-
10	80	-	-	-	-	100	100	99.9	96.1	77.8
20	98	-	-	-	-	100	100	100	100	99.2
30	100	64.4	-	-	-	100	100	100	100	100

Table 35 Accuracy of the assessment Joint 5 (DC-2, Model 2)

Simulation	Accuracy of the assessment using Joint 5 (%)									
	Damage = 15%					Damage = 35%				
	ε (%)					ε (%)				
	1	2	3	4	5	1	2	3	4	5
1	-	-	-	-	-	96.1	-	-	-	-
10	70.9	-	-	-	-	100	99.8	94.7	73.1	-
20	97.6	-	-	-	-	100	100	99.5	96.3	87.4
30	99.7	-	-	-	-	100	100	99.9	99.4	96.4

Table 36 Accuracy of the assessment Joint 6 (DC-2, Model 2)

Simulation	Accuracy of the assessment using Joint 6 (%)									
	Damage = 15%					Damage = 35%				
	ε (%)					ε (%)				
	1	2	3	4	5	1	2	3	4	5
1	-	-	-	-	-	-	-	-	-	-
10	-	-	-	-	-	99.9	73	-	-	-
20	-	-	-	-	-	100	97	62.9	-	-
30	-	-	-	-	-	100	100	84.7	53.9	-

Table 37 Accuracy of the assessment using the average of the joints (DC-2, Model 2)

Simulation	Accuracy of the assessment using average of joint 2,3,4,5, & 6 (%)									
	Damage = 15%					Damage = 35%				
	ε (%)					ε (%)				
	1	2	3	4	5	1	2	3	4	5
1	-	-	-	-	-	100	-	-	-	-
10	88	-	-	-	-	100	100	100	99.4	-
20	100	-	-	-	-	100	100	100	100	100
30	100	52.9	-	-	-	100	100	100	100	100

Table 38 The average of the severity estimation Joint 3 (subset data, DC-2, Model 2)

Simulation	The Average of the severity estimation Joint 3 (%)									
	Damage = 15%					Damage = 35%				
	ε (%)					ε (%)				
	1	2	3	4	5	1	2	3	4	5
1	-	-	-	-	-	34.9	34.5	-	-	-
10	14.6	14.5	-	-	-	35	35	34.9	34.8	34.7
20	14.6	14.5	14.5	-	-	35	35	34.9	34.9	34.9
30	14.6	14.5	14.5	14.5	-	35	35	35	34.9	34.9

5.2.2.3 Cross-Section Damage in element 43: DC-3 Model 2

In this damage case, element 43, shown in Figure 4c, is simulated to be damaged due to a reduction in the cross-sectional area by 15% and 35%, along with the entire length. It is noticeable from Figure 13 that there are two spikes at Joints 3 and 4, illustrating that Joints 3 and 4 are the most accurate joints to estimate the severity of the damage among all other joints; even so, Joint 4 is slightly more accurate than Joint 3, since the absolute difference of the contribution between the damaged and undamaged state when the static moving load at Joint 4 is greater than when it is at Joint 3. However, in this case, Joint 4 is not the most sensitive joint for the damage localization method, and the cause might be that the damaged member experience both compression and tension forces. The results of joints 3 and 4 in Figure 13 are matching and Joints 2 and 5 as well. It is shown that at 15%, all the assessment procedures indicate damage with number of simulations 10, 20, and 30 and levels of noise 1% to 3%, while at 35% severity the damage assessment using the displacement data of Joint 2 detect the damage element with one simulation and up to the

3% level of noise, whereas utilizing Joints 3, 4, 5, and the average of the joints assessment approaches identify the damage at the noise level of 1%. The average of severity estimations of the corresponding considerations of the damage location using Joint 4 subset displacement data (55 ft – 80 ft away from the left support) shows accurate results with a maximum absolute error of 0.2% and 1.9% for damage severity of 15% and 35%, respectively, shown in table 44. Overall, the damaged element is detected and relatively quantified using the displacement data of Joint 4 at some levels of noise and number of simulations for the severity of 15% and 35%.

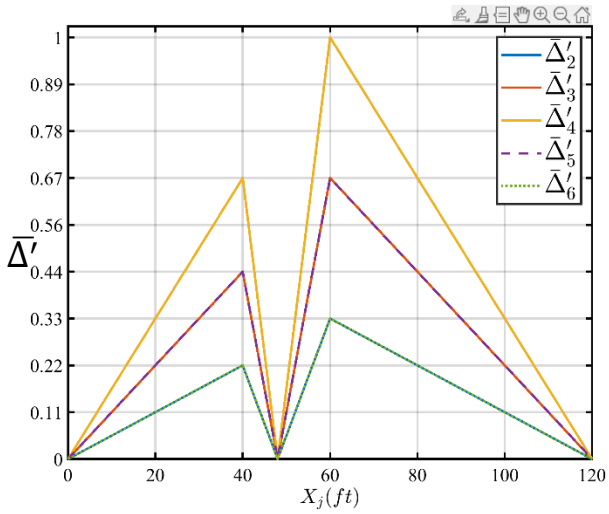

Figure 13 Location of the maximum contribution from the damaged member to the bottom chord joints (DC-3, Model 2)

Table 39 Accuracy of the assessment Joint 2 (DC-3, Model 2)

Simulation	Accuracy of the assessment using Joint 2 (%)									
	Damage = 15%					Damage = 35%				
	ε (%)					ε (%)				
	1	2	3	4	5	1	2	3	4	5
1	-	-	-	-	-	95.1	78.3	51.4	-	-
10	60.6	-	-	-	-	100	99.1	95.6	88.3	72.4
20	77.8	-	-	-	-	100	99.8	98.8	95.7	91.9
30	85.7	55.9	-	-	-	100	100	99.4	98.3	96.7

Table 40 Accuracy of the assessment Joint 3 (DC-3, Model 2)

Simulation	Accuracy of the assessment using Joint 3 (%)									
	Damage = 15%					Damage = 35%				
	ε (%)					ε (%)				
	1	2	3	4	5	1	2	3	4	5
1	-	-	-	-	-	92.1	-	-	-	-
10	81.8	-	-	-	-	100	99.6	92.2	68.7	-
20	97.8	50.9	-	-	-	100	100	99	94.2	80.5
30	99.2	70	-	-	-	100	100	99.9	98.3	93.3

Table 41 Accuracy of the assessment Joint 4 (DC-3, Model 2)

Simulation	Accuracy of the assessment using Joint 4 (%)									
	Damage = 15%					Damage = 35%				
	ε (%)					ε (%)				
	1	2	3	4	5	1	2	3	4	5
1	-	-	-	-	-	98.3	-	-	-	-
10	70.5	-	-	-	-	100	100	97.2	78.6	
20	82.3	59.1	-	-	-	100	100	100	98.3	88.8
30	89.5	65.3	-	-	-	100	100	100	99.7	96.9

Table 42 Accuracy of the assessment Joint 5 (DC-3, Model 2)

Simulation	Accuracy of the assessment using Joint 5 (%)									
	Damage = 15%					Damage = 35%				
	ε (%)					ε (%)				
	1	2	3	4	5	1	2	3	4	5
1	-	-	-	-	-	90.2	-	-	-	-
10	79.5	-	-	-	-	100	99	87.5	58.9	-
20	97	47.9	-	-	-	100	100	99.1	91.8	72.8
30	99.4	65.3	-	-	-	100	100	99.8	97.5	91

Table 43 Accuracy of the assessment Joint 6 (DC-3, Model 2)

Simulation	Accuracy of the assessment using Joint 6 (%)									
	Damage = 15%					Damage = 35%				
	ε (%)					ε (%)				
	1	2	3	4	5	1	2	3	4	5
1	-	-	-	-	-	93.7	77.8	-	-	-
10	74.5	-	-	-	-	100	98.4	94	86.1	70.5
20	88	60.4	-	-	-	100	100	98.4	94.2	90.9
30	94	69.5	51.3	-	-	100	100	99.3	97	94.6

Table 44 Accuracy of the assessment using the average the joints (DC-3, Model 2)

Simulation	Accuracy of the assessment using average of joint 2,3,4,5, & 6 (%)									
	Damage = 15%					Damage = 35%				
	ε (%)					ε (%)				
	1	2	3	4	5	1	2	3	4	5
1	-	-	-	-	-	100	-	-	-	-
10	92	-	-	-	-	100	100	100	96.1	59.8
20	100	58	-	-	-	100	100	100	100	99.4
30	100	80	-	-	-	100	100	100	100	100

Table 45 The average of the severity estimation Joint 4 (subset data, DC-3, Model2)

Simulation	The Average of the severity estimation Joint 4 (%)									
	Damage = 15%					Damage = 35%				
	ε (%)					ε (%)				
	1	2	3	4	5	1	2	3	4	5
1	-	-	-	-		33.8	-	-	-	-
10	15	-	-	-	-	34.7	34.4	33.9	33.1	-
20	15.1	14.8	-	-	-	34.8	34.6	34.4	34	33.5
30	15.1	14.9	-	-	-	34.8	34.7	34.5	34.3	34

5.2.2.4 Cross-Section Damage in element 23: DC-4 Model 2

In this damage case, element 23, shown in Figure 4b, is simulated to be damaged due to a reduction in the cross-sectional area by 15% and 35%, along with the entire length. It is observed from tables 47 and 49 that the damage assessments using displacement data of Joints 3 and 5 detect the damage only at 35% severity. It is recognizable that at one simulation, both assessments identify damage only at 1% of noise level, while with 20 and 30 simulations, the damage assessments can locate the damage up to 5% of noise due to increasing the data which leading to improve the accuracy. It is remarkable from Figure 14 that Joint 4 is the most sensitive joint to the damaged member, so it is observed that the damage is located at 15% severity with 10 simulations at only 1% level of noise. The average severity using displacement data of Joint 4 is shown in table 52. The subset data is considered when the moving load in between 40ft -80ft away from the left support. The results show that the severity is accurately assessed with a maximum absolute error of 0.3% and 0.4% for the severity level of 15% and 35%, respectively, for the detected cases in

table 47. Overall, the existence of the damage in element 23 is detected and localized at the severity of 15% and 35% using Joint 4 and the average assessment at some level of noise and number of simulations

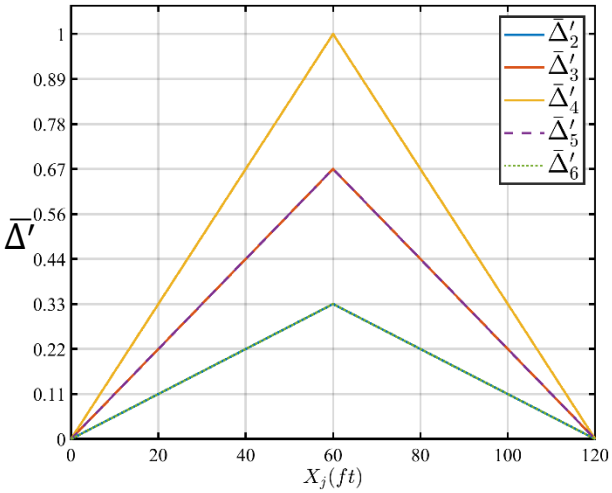

Figure 14 Location of the maximum contribution from the damaged member to the bottom chord joints (DC-4, Model 2)

Table 46 Accuracy of the assessment Joint 2 (DC-4, Model 2)

Simulation	Accuracy of the assessment using Joint 2 (%)									
	Damage = 15%					Damage = 35%				
	ε (%)					ε (%)				
	1	2	3	4	5	1	2	3	4	5
1	-	-	-	-	-	-	-	-	-	-
10	66.9	-	-	-	-	67.6	-	-	-	-
20	97.4	-	-	-	-	84	50.4		-	-
30	99.6	-	-	-	-	92.8	59.8	-	-	-

Table 47 Accuracy of the assessment Joint 3 (DC-4, Model 2)

Simulation	Accuracy of the assessment using Joint 3 (%)									
	Damage = 15%					Damage = 35%				
	ε (%)					ε (%)				
	1	2	3	4	5	1	2	3	4	5
1	-	-	-	-	-	93.4	-	-	-	-
10	-	-	-	-	-	100	99.8	92.6	63.8	-
20	-	-	-	-	-	100	100	99.6	94.6	81.3
30	-	-	-	-	-	100	100	100	99.2	94.8

Table 48 Accuracy of the assessment Joint 4 (DC-4, Model 2)

Simulation	Accuracy of the assessment using Joint 4 (%)									
	Damage = 15%					Damage = 35%				
	ε (%)					ε (%)				
	1	2	3	4	5	1	2	3	4	5
1	-	-	-	-	-	100	-	-	-	-
10	100	-	-	-	-	100	100	99.3	92.8	68.7
20	100	86.2	-	-	-	100	100	100	99.8	96.6
30	100	98.1	54.4	-	-	100	100	100	100	99.7

Table 49 Accuracy of the assessment Joint 5 (DC-4, Model 2)

Simulation	Accuracy of the assessment using Joint 5 (%)									
	Damage = 15%					Damage = 35%				
	ε (%)					ε (%)				
	1	2	3	4	5	1	2	3	4	5
1	-	-	-	-	-	94.1	-	-	-	-
10	-	-	-	-	-	100	99.8	92.9	65.2	-
20	-	-	-	-	-	100	100	99.3	95.5	80.7
30	-	-	-	-	-	100	100	100	98.9	93.8

Table 50 Accuracy of the assessment Joint 6 (DC-4, Model 2)

Simulation	Accuracy of the assessment using Joint 6 (%)									
	Damage = 15%					Damage = 35%				
	ε (%)					ε (%)				
	1	2	3	4	5	1	2	3	4	5
1	-	-	-	-	-	-	-	-	-	-
10	67.6	-	-	-	-	67.1	-	-	-	-
20	97	-	-	-	-	84.8	50.2	-	-	-
30	99.8	-	-	-	-	92.9	59.3	-	-	-

Table 51 Accuracy of the assessment using the average the joints (DC-4, Model 2)

Simulation	Accuracy of the assessment using average of Joint 2,3,4,5, & 6 (%)									
	Damage = 15%					Damage = 35%				
	ε (%)					ε (%)				
	1	2	3	4	5	1	2	3	4	5
1	-	-	-	-	-	98.7	-	-	-	-
10	93.3	-	-	-	-	100	100	98.7	55.6	-
20	100	-	-	-	-	100	100	100	99.7	85.3
30	100	75	-	-	-	100	100	100	100	99.2

Table 52 The average of the severity estimation Joint 4 (subset data, DC-4, Model2)

Simulation	The Average of the severity estimation Joint 4 (%)									
	Damage = 15%					Damage = 35%				
	ε (%)					ε (%)				
	1	2	3	4	5	1	2	3	4	5
1	-	-	-	-	-	34.8	-	-	-	-
10	14.8	-	-	-	-	34.9	34.9	34.8	34.8	34.6
20	14.8	14.8	-	-	-	34.9	34.9	34.9	34.8	34.8
30	14.8	14.8	14.7	-	-	34.9	34.9	34.9	34.9	34.9

CHAPTER 6

CONCLUSION AND FUTURE WORK

This thesis outlines a theoretical framework for the utilization of displacement influence lines of the bottom chord joints calculated from a moving unit load for damage localization and severity estimation of a single damaged member on steel truss bridge. The relation between the absolute normalized difference of the DILs and absolute normalized axial force influence lines of the damaged member is shown as MSE equation 8. The severity estimation is presented in equation 11 which is based on the contribution ratio of the damaged member to the vertical displacement of each joint.

To overcome the challenges with noisy measurements to the damage localization method, the number of moving load steps is increased, while the accuracy of the severity estimation is improved by considering a subset of displacement data after detecting the damaged member by calculating the maximum contribution from the damaged member to the bottom chord joints, as shown and compared in DC -1, DC -2, and DC -3 for Model 1. To validate the proposed method, analytical studies in various combinations of noise level, number of simulations, and damage severity have been provided.

Specific conclusions and contributions for this study include the following:

- The relationship between the vertical displacement influence lines of the bottom chord joints and changes in the axial rigidity of the truss elements has been established for determinant structures

- The accuracy of the proposed method is a function of the damage severity, level of noise, number of simulations, and sensitivity of the bottom chord joints to the damaged member.
- The proposed theory can localize and characterize damage in truss members with relatively few sensors by using the static displacement influence lines at some combinations of noise level, number of simulations, damage location, and severity for different types of truss bridges.
- The proposed method is not applicable for zero-force members
- Two members or more may have the same normalized axial force influence lines, so if damage occurred in one of these members, the proposed damage would indicate damage in all these members.

Future Work:

In the future, it is planned to validate the results in a laboratory-scale and Enhance the accuracy and performance of the proposed method by considering both flexural and axial rigidity in the calculation for truss bridges with different joint connections stiffnesses. In addition to expand the proposed method to characterize damage in multiple, simultaneously impaired members.

APPENDIX A

NOTATION LIST

J	Number of the moving load steps
M	Number of the truss members
N	Number of the bottom chord joints
j	Location of the moving load
n	Location of the measurements
M	Member
Δ	Is [J*N] matrix represents the DILs of the bottom chord joints.
F	Is [J*M] matrix represents the AFILs for the truss members due to a real moving load.
K	Is [M*M] diagonal matrix, on-diagonal entries represent the axial stiffnesses of the truss members.
Q	Is [M*N] matrix represents the AFILs of the truss members due to a unit moving load.
C	Is [M*N] matrix represents the influence line coefficients for the truss members.
I	Is [N*N] identity matrix.
xj	The location of the moving load
$P_{n(xj)}$	Is the amount of the moving load transferred to joint n when the load is at xj

Δ'	The difference between the damaged and intact SDILs of the bottom chord joints
Δ^d	SDILs of the damaged bridge
$\overline{\Delta'_n}$	The absolute normalized difference between the SDILs of the intact and damaged bridge
$\overline{F_m}$	The normalized AFIL of member m
C_m	The coefficients influence lines of member m
CR_{jnm}	The contribution ratio of the axial displacement of member m to the vertical deflections of joint n when the real moving load at j
Δ^c_{jn}	The calculated vertical displacement
$SE\%_m$	Severity estimation for the damage in member m
Δ_{noisy}	Is the noisy SDILs
$\Delta_{noise-free}$	Is the free noise SDILs
ε	Level of noise
R	A matrix that has the same size as the $\Delta_{noise-free}$ and R contains random numbers in the range [-1 1]

References

[1] ASCE. (2021). *2021 Report Card for America's Infrastructure*. Retrieved from https://infrastructurereportcard.org/.

[2] Story, Brett Alan. *Structural impairment detection using arrays of competitive artificial neural networks*. Texas A&M University, 2012.

[3] Chang, Kai-Chun, and Chul-Woo Kim. "Modal-parameter identification and vibration-based damage detection of a damaged steel truss bridge." *Engineering Structures* 122 (2016): 156-173.

[4] Nuno, Kazuma. "Damage detection of a steel truss bridge using frequency response function curvature method." (2013).

[5] Kim, C. W., S. Kitauchi, and K. Sugiura. "Damage detection of a steel truss bridge through on-site moving vehicle experiments." *SMAR-2nd International Conference on Smart Monitoring, Assessment and Rehabilitation of Civil Structures, Istanbul, Turkey*. 2013.

[6] Guo, H. Y. "Structural damage detection using information fusion technique." *Mechanical Systems and Signal Processing* 20.5 (2006): 1173-1188.

[7] Mustafa, Samim, Yasunao Matsumoto, and Hiroki Yamaguchi. "Vibration-based health monitoring of an existing truss bridge using energy-based damping evaluation." *Journal of Bridge Engineering* 23.1 (2018): 04017114.

[8] Siriwardane, Sudath C. "Vibration measurement-based simple technique for damage detection of truss bridges: A case study." *Case Studies in Engineering Failure Analysis* 4 (2015): 50-58.

[9] Boumechra, Nadir. "Damage detection in beam and truss structures by the inverse analysis of the static response due to moving loads." *Structural Control and Health Monitoring* 24.10 (2017): e1972.

[10] Jang, S. A., S. H. Sim, and B. F. Spencer Jr. "Structural damage detection using static strain data." *Proceedings of the World Forum on Smart Materials and Smart Structures Technology, China*. 2007.

[11] Bakhtiari-Nejad, F., A. Rahai, and A. Esfandiari. "A structural damage detection method using static noisy data." *Engineering structures* 27.12 (2005): 1784-1793.

[12] Lee, Eun-Taik, Hee-Chang Eun, and Tae-Wan Kim. "622. Damage detection of truss structure based on the variation in axial stress and strain energy predicted from incomplete measurements." (2011).

[13] Graybeal, Benjamin A., et al. "Visual inspection of highway bridges." *Journal of nondestructive evaluation* 21.3 (2002): 67-83.

[14] The study, conducted by the U.S. Federal Highway Administration's Nondestructive Evaluation Validation Center (NDEVC) in 2001, investigated the accuracy and reliability of routine and in-depth visual inspections.

[15] Rytter, Anders. "Vibrational based inspection of civil engineering structures." (1993).

[16] Brunell, Garrett, and Yail J. Kim. "Effect of local damage on the behavior of a laboratory-scale steel truss bridge." *Engineering structures* 48 (2013): 281-291.

[17] Hajizeinalibiouki, Yasha. "Flexural Rigidity Estimation Using Noisy Static Influence Lines." (2018).

[18] Zeinali, Yasha, and Brett A. Story. "Framework for flexural rigidity estimation in Euler-Bernoulli beams using deformation influence lines." *Infrastructures* 2.4 (2017): 23.

[19] Chen, Zhi-Wei, et al. "Damage detection in long suspension bridges using stress influence lines." *Journal of Bridge Engineering* 20.3 (2015): 05014013.

[20] Bernal, Dionisio. "Damage localization and quantification from the image of changes in flexibility." *Journal of Engineering Mechanics* 140.2 (2014): 279-286.

[21] Zaurin, R., and F. N. Catbas. "Integration of computer imaging and sensor data for structural health monitoring of bridges." *Smart Materials and Structures* 19.1 (2009): 015019.

[22] Zaurin, Ricardo, and F. Necati Catbas. "Structural health monitoring using video stream, influence lines, and statistical analysis." *Structural Health Monitoring* 10.3 (2011): 309-332.

[23] Catbas, F. Necati, et al. "Integrative information system design for Florida Department of Transportation: A framework for structural health monitoring of movable bridges." (2007).

[24] Catbas, F. Necati, et al. "Sensor networks, computer imaging, and unit influence lines for structural health monitoring: Case study for bridge load rating." *Journal of Bridge Engineering* 17.4 (2012): 662-670.

[25] Zaurin, R.; Khuc, T.; Catbas, F. Hybrid sensor-camera monitoring for damage detection: Case study of a real bridge. J. Bridge Eng. 2016, 21.

[26] Turer, Ahmet. *Condition evaluation and load rating of steel stringer highway bridges using field calibrated 2D-grid and 3D-FE models*. Diss. University of Cincinnati, 2000.

[27] Aktan, A. E., A. Turer, and A. Levi. *INSTRUMENTATION, PROOF-TESTING AND MONITORING OF THREE REINFORCED CONCRETE DECK-ON-STEEL GIRDER BRIDGES PRIOR TO, DURING, AND AFTER SUPERLOAD*. No. FHWA/OH-98/015,. 1998.

[28] Zeinali, Yasha, and Brett A. Story. "Impairment localization and quantification using noisy static deformation influence lines and Iterative Multi-parameter Tikhonov Regularization." *Mechanical Systems and Signal Processing* 109 (2018): 399-419.

[29] Štimac-Grandić, Ivana. "Influence of sampling interval on deflection-influence-line-based damage detection in beams." *Journal of Applied Engineering Science* 12.1 (2014): 69-74.

[30] Štimac, Ivana, Ante Mihanović, and Ivica Kožar. "„Damage Detection from Analysis of Displacement Influence Lines “." *International Conference on Bridges, Dubrovnik*. 2006.

[31] Wang, Chung-Yue, Chin-Kuo Huang, and Chin-Shian Chen. "Damage assessment of beam by a quasi-static moving vehicular load." *Advances in Adaptive Data Analysis* 3.04 (2011): 417-445.

[32] Wang, Y. L., and X. L. Liu. "Beam damage localization method considering random uncertainty using mid-span displacement data." *Sustainable Development of Critical Infrastructure*. 2014. 438-446.

[33] Kourehli, S. S. "Structural damage diagnosis using incomplete static responses and LS-SVM." *Inverse Problems in science and engineering* 25.3 (2017): 418-433.

[34] Sitton, Jase D., Yasha Zeinali, and Brett A. Story. "Design and field implementation of an impact detection system using committees of neural networks." *Expert Systems with Applications* 120 (2019): 185-196.